



**HAL**  
open science

## Three states and three steps simulated within Ising like model solved by local mean field approximation in 3D spin crossover nanoparticles

Catherine Cazelles, Yogendra Singh, Jorge Linares, Pierre-Richard Dahoo,  
Kamel Boukheddaden

### ► To cite this version:

Catherine Cazelles, Yogendra Singh, Jorge Linares, Pierre-Richard Dahoo, Kamel Boukheddaden. Three states and three steps simulated within Ising like model solved by local mean field approximation in 3D spin crossover nanoparticles. *Materials Today Communications*, 2021, 26 (March), pp.102074. 10.1016/j.mtcomm.2021.102074 . insu-03130819

**HAL Id: insu-03130819**

**<https://insu.hal.science/insu-03130819>**

Submitted on 4 Feb 2021

**HAL** is a multi-disciplinary open access archive for the deposit and dissemination of scientific research documents, whether they are published or not. The documents may come from teaching and research institutions in France or abroad, or from public or private research centers.

L'archive ouverte pluridisciplinaire **HAL**, est destinée au dépôt et à la diffusion de documents scientifiques de niveau recherche, publiés ou non, émanant des établissements d'enseignement et de recherche français ou étrangers, des laboratoires publics ou privés.

# Journal Pre-proof

Three states and three steps simulated within Ising like model solved by local mean field approximation in 3D spin crossover nanoparticles

Catherine Cazelles (Software) (Writing - original draft), Yogendra Singh (Software) (Writing - original draft), Jorge Linares (Conceptualization) (Methodology) (Project administration) (Writing - review and editing) (Software), Pierre-Richard Dahoo (Software) (Writing - review and editing), Kamel Boukheddaden (Conceptualization) (Methodology) (Project administration) (Writing - review and editing)



PII: S2352-4928(21)00066-0

DOI: <https://doi.org/10.1016/j.mtcomm.2021.102074>

Reference: MTCOMM 102074

To appear in: *Materials Today Communications*

Received Date: 23 December 2020

Revised Date: 20 January 2021

Accepted Date: 20 January 2021

Please cite this article as: Cazelles C, Singh Y, Linares J, Dahoo P-Richard, Boukheddaden K, Three states and three steps simulated within Ising like model solved by local mean field approximation in 3D spin crossover nanoparticles, *Materials Today Communications* (2021), doi: <https://doi.org/10.1016/j.mtcomm.2021.102074>

This is a PDF file of an article that has undergone enhancements after acceptance, such as the addition of a cover page and metadata, and formatting for readability, but it is not yet the definitive version of record. This version will undergo additional copyediting, typesetting and review before it is published in its final form, but we are providing this version to give early visibility of the article. Please note that, during the production process, errors may be discovered which could affect the content, and all legal disclaimers that apply to the journal pertain.

© 2020 Published by Elsevier.

## Three states and three steps simulated within Ising like model solved by local mean field approximation in 3D spin crossover nanoparticles

Catherine Cazelles <sup>a</sup>, Yogendra Singh <sup>b</sup>, Jorge Linares <sup>b,c\*</sup>, Pierre-Richard Dahoo <sup>d</sup>, Kamel Boukheddaden <sup>b\*</sup>

<sup>a</sup> Université Paris-Saclay, UVSQ, IUT de Mantes-en-Yvelines, 78200 Mantes-la-Jolie

<sup>b</sup> Université Paris-Saclay, UVSQ, CNRS, GEMaC, 78000 Versailles, France

<sup>c</sup> Departamento de Ciencias, Sección Física, Pontificia Universidad Católica del Perú, Apartado 1761 - Lima, Peru

<sup>d</sup> Université Paris-Saclay, UVSQ, CNRS, LATMOS, 78280 Guyancourt, France

\*Corresponding authors : jorge.linares@uvsq.fr, kamel.boukheddaden@uvsq.fr

### ABSTRACT

Coordination iron (II) compounds are studied to simulate switching properties between low spin (LS,  $S=0$ ) and high-spin (HS,  $S=2$ ) states in spin-crossover materials. These two states are diamagnetic (LS) and paramagnetic (HS) in nature, and the switching between these two states is achieved through external excitations which may be of thermal or of pressure origin. In this contribution, a local mean-field approach is proposed to study SCO nano/micro-particles, for which distinctions among the contributions of molecules localized at the edge, corner, surface or the bulk, as well as for the external coupling that concerns only surface particles have been introduced. In this first attempt, the model is solved using a rough approximation which simplifies its treatment, leading to finding out three steps switching and three states, simulated under temperature effect while two steps transitions are obtained under pressure effect.

**Keywords:** Ising-like model / Local mean-field approximation / spin crossover / nanoparticles or micro-particles/ surface effects.

### 1. INTRODUCTION

Spin crossover (SCO) compounds could be considered as text-book examples of molecular systems, which have uncanny ability to reversibly switch from a high spin (HS) to a low spin (LS) state [1-4] and can act under a wide range of external stimuli such as temperature [5-8], pressure [9-11], electrical, magnetic [12] or photo- excitations [13-18]. The phenomenon is in general followed by some of its signature behaviors, like variations in the magnetic, optical, structural and electrical properties of the material. In its solid state, given that one of the widely studied stimuli for LS-HS transition is temperature, the thermal properties of the SCO materials may give rise to a very rich set of behaviors which include (i) continuous gradual spin-transitions (Boltzmann population of two degenerate states) (ii) sharp first-order transitions, ranging from (iii) incomplete transitions (non-zero HS fraction at lower temperatures) to (iv) two or multi-step spin transitions. The final result could be either of these transition paths or some mix of these transition paths. Due to such richness of variety, SCO systems have been studied for many years. Their applications are considered as very promising such as data storage, displays, pressure sensors, and molecular switches.

There are multiple reasons and multiple ways which may give rise and govern these behaviors in SCO compounds: (i) multi-stability or/and the existing structural ordering in the

molecule itself (binuclear SCO systems). (ii) asymmetry, having two or more non-equivalent sites. (iii) through architecture (SCO core-shell nanocomposites). (iv) different local environments (surface effects) i.e. size reduction. However, compounds exhibiting multistep spin conversion had remained quite elusive and rare, but since last decade this field has garnered increasing attention in both theoretical and experimental aspects, due to their promising application in 3-bit electronics. Thus, it is worth considering that the processing of SCO materials with two inequivalent sites is hardly controllable, and thus makes the behavior of the high-spin fraction highly unpredictable. Recently, chemists started designing well controllable and reproducible SCO core-shell nanocomposites, but it is still nascent and might lead to instability due to large structural changes at the interface [19].

Despite the difficulties and challenges faced, the prospects of multistep transition are promising. With the growing interest in the nanoscale phenomenon, advances in visualization and design are taking place rapidly, thanks to the state-of-art experimental tools (electronic and atomic force microscopy, high-resolution x-ray diffraction) along with the usual detection techniques (Optical spectroscopy, Mossbauer, Magnetometry, Dielectric constant, Calorimetry [20] etc.). To boost the development of nanotechnologies and the availability of experimental results, a theoretical viewpoint is also required because the synergy between theoretical and experimental studies enhances and optimizes research activities at the nanoscale. Surface relaxations and effects may play a major role in this case, in order to understand phenomena in new SCO nano-objects, such as thin films, nanoparticles and nanopatterns, where surface geometry plays a major or deterministic role. Therefore, understanding the dynamics of the size reduction and its effects on the spin transition has become of paramount importance.

The experimental observations are already indicative of a variety of finite-size effects in different SCO compounds. These effects may originate from different causes such as the structural diversity of these materials, due to mono-, poly-nuclear compounds, or the numerous physico-chemical phenomena which can arise due to surface, confinement and kinetic effects. However, as one keeps on downsizing, decrease in cooperativity, incomplete transitions and in general, a shift in transition temperatures toward the low-temperature end can be observed. All these trends could be explained by taking into account simple thermodynamical considerations which indicate higher surface energy in the LS state, and thus leading to stabilization of HS state on surfaces even at low temperatures.

This idea was also supported by investigations conducted in 2D microscopic Monte Carlo simulations using Local Mean Field Approximation (LMFA), which clearly depict that the number of molecules at the surface or corners with the different number of neighbors becomes extensively important and could not be ignored [21]. In SCO compounds, edge, corner and bulk environments are physical distinct realities. It must be recalled that in these compounds, the active spin site which is due to the presence of a 3d transition element such as an iron cation ( $\text{Fe}^{2+}$  or  $\text{Fe}^{3+}$ ) is interacting through the local ligand field either directly or indirectly through the chemical bonds with a number of different atoms which may be carbon, nitrogen or others elements composing the matrix in which the cation is embedded. In this respect, the study was particularly interesting as it shed light on the appearance of two-step transition due to the thermodynamic interplay among the bulk, edge and corner molecules.

In this paper, the previous model [22,23] has been extended to investigate 3D SCO in detail and to understand the role of surface relaxations in transitions. The Ising-like model is used and solved in the framework of the Local Mean Field Approximation (LMFA) to study

both shape and size effects on the 3D SCO compounds. This LMFA is better adapted to the present study to reproduce thermal and pressure hysteresis with access to metastable states than Monte Carlo-Metropolis technique that is well adapted to study metastable states.

## 2. MODEL AND PRINCIPLE OF CALCULATION

Wajnflasz and Pick [22] developed in 1970 the first microscopic Ising-like model in which only short-range interactions were taken into account for studying the spin transition behavior. This model was later adapted by Bousseksou *et al.* [23] in the frame of the mean-field approximation to simulate two-steps transitions. B. Hoo *et al.* [24] make the first extension of this Ising-like model to take into account the next-nearest neighbors. Linares *et al.* [25] showed that it was necessary to add long-range interactions to reveal a transition with hysteresis in 1D compounds. The dynamic of this short- and long-interaction model has been treated by K. Boukheddaden *et al.* [26]. Later on, a new interaction term “L” has been introduced in the Hamiltonian to take into account the influence of the environment (matrix effect) [27-29].

Thanks to these previous contributions, the Hamiltonian can be expressed as follows:

$$H = \frac{\Delta - k_B T \ln g}{2} \sum_{i=1}^{N_T} \sigma_i - J \sum_{\langle i,j \rangle} \sigma_i \sigma_j - G \sum_{i=1}^{N_T} \sigma_i \langle \sigma \rangle - \sum_{i=1}^M L_i \sigma_i \quad (1)$$

In equation (1), the first term is the sum of the contributions of each isolated molecules and  $N_T$  denotes the total number of molecules. The ligand field  $\Delta$  ( $> 0$ ) is the energy difference between the high spin (HS) and the low spin (LS) configurations and  $g = g_{HS}/g_{LS}$  is the degeneracy ratio between (HS) and (LS) energy levels which takes into account, not only the degenerations of electronic origin but also the degenerations of vibrational origin.  $T$  is the absolute temperature and  $k_B$  is the Boltzmann constant such as  $\beta = 1/(k_B T)$ .  $\sigma$  is a fictitious spin operator whose eigenstates are +1 and -1 respectively associated to the high-spin (HS) and low-spin (LS) states [8-10]. The second term accounts for the coupling  $J$  between the nearest-neighbor spin pairs  $\langle i, j \rangle$ . The third term  $G$  is the long-range part of the interaction and the last term  $L_i$  expresses the sum of the contributions of negative local ligand-field felt by the molecules located on the outline of the compound due to their interactions with the surrounding. Here, the magnitude of this field is clearly distinguished according to the position of the molecules (edge, corner or surface), while this field vanishes for the bulk molecules.

In order to develop a general approach to solve such problems, existence of four regions in the lattice (bulk, edge, corner, surface), can be expected to have four corresponding coupled order parameters associated with each of these regions. Indeed, a realistic approach to this problem in the local mean-field framework leads to re-express Hamiltonian (1) under the following form:

$$H = \frac{\Delta - k_B T \ln g}{2} \sum_{i=1}^{N_T} \sigma_i - J \sum_{\langle i,j \rangle} \sigma_i q_i \langle \sigma \rangle_i - G \sum_{i=1}^{N_T} \sigma_i \langle \sigma \rangle - \sum_{i=1}^M L_i \sigma_i \quad (2)$$

where  $\langle \sigma \rangle_i$  is the average spin state around site  $i$  and  $q_i$  is its coordination number.

Assuming that the local average order parameter  $\langle \sigma \rangle_i$  contains four types of homogeneous contributions,  $\langle \sigma \rangle_b$ ,  $\langle \sigma \rangle_c$ ,  $\langle \sigma \rangle_e$ ,  $\langle \sigma \rangle_s$  corresponding respectively to bulk, corner, edge and surface contributions, it becomes possible to solve the statistical-mechanics problem

which leads to four non-linear coupled equations. This approach will be developed in further work where the rigorous variational calculations will be developed.

In the present contribution, to oversimplify the problem it is assumed that the contributions of the short and long-range parameters ( $-J \sum_{\langle i,j \rangle} \sigma_i \sigma_j - G \sum_{i=1}^{N_T} \sigma_i \langle \sigma \rangle$ ) can be merged into the same energetic contribution, written under the following form:

$$-\Gamma \langle \sigma \rangle \sum_{i=1}^{N_T} q_i \sigma_i \quad (3)$$

where the only local information kept is that of the coordination number of the considered site. On the other hand, the new parameter  $\Gamma$  must be seen as a control parameter and not as a variational parameter which depends on  $J$  and  $G$ . Therefore, from now, all thermal properties will be investigated using the coupling parameters,  $\Gamma$  and  $L_i$ . In this work,  $\Gamma$  will be considered as positive quantity, thus favoring ferromagnetic-like interactions, i.e. (HS)-(HS) and (LS)-(LS) pairs, whereas (HS)-(LS) pairs are favored when  $\Gamma$  is negative (anti-ferromagnetic-like interactions). It is interesting to mention that although the case  $\Gamma < 0$  is not considered here, it might be interesting to investigate this case corresponding to dominant long-range antiferromagnetic like interactions.

Accepting the sacrifice of the approximation made in (3), the total Hamiltonian of the system can be re-written as follows:

$$H = \frac{\Delta - k_B T \ln g}{2} \sum_{i=1}^{N_t} \sigma_i - \Gamma \langle \sigma \rangle \sum_{i=1}^{N_T} q_i \sigma_i - \sum_{i=1}^M L_i \sigma_i \quad (4)$$

In the frame of a classical mean-field approximation and the case of a 3D cubic lattice, the coordination number is  $q = 6$  (see Fig. 1).

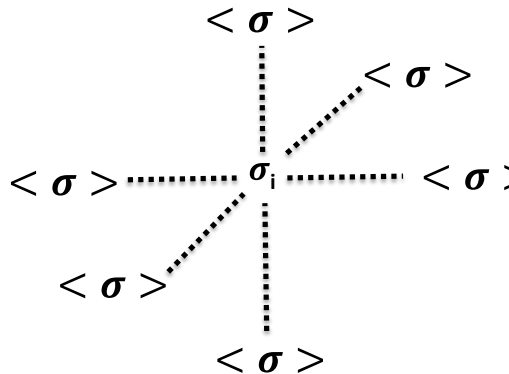


**Fig. 1.** Mean-field approximation in a 3D cubic lattice:  $\sigma_i$  spin surrounded by 6 nearest-neighbor with the average magnetization  $\langle \sigma \rangle$ .

It is important to remember that while dealing with nanoparticles, surface properties can play a significant role and deeply modify the material properties. In order to include rigorously the matrix effects, it is to be considered that the number of bonds for the molecules inside the lattice is different from the one for molecules outside the lattice.

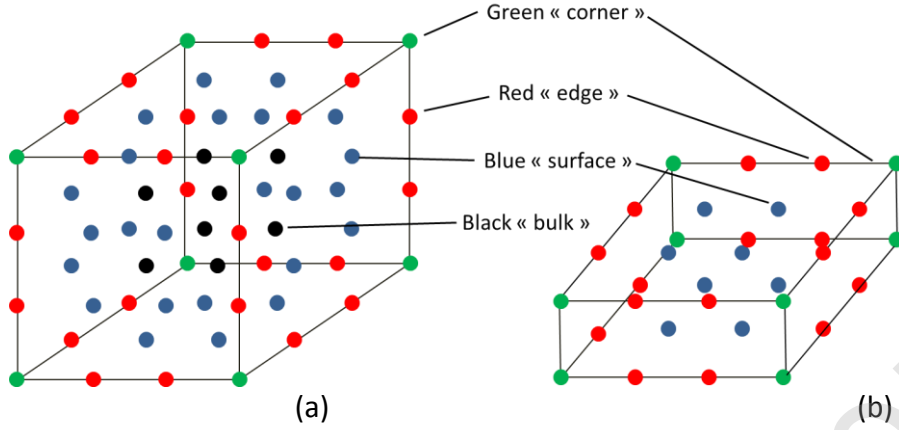


**Fig. 2.** Schematic view of the 3D lattices of two SCO nanoparticles: filled black circles represent bulk sites ( $N_b$ ), while filled blue, red and green circles represent respectively surface ( $N_s$ ), edge ( $N_e$ ) and corner ( $N_c$ ) sites which have interactions with their immediate environment. (a)  $N_x \times N_y \times N_z$  cubic lattice with size  $4 \times 4 \times 4$  (b)  $N_x \times N_y \times N_z$  parallelepiped lattice with size  $4 \times 4 \times 2$ .

As seen in Fig. 2, four types of sites have to be considered: molecules located in the bulk  $N_b$ , on the surface  $N_s$ , on the edge  $N_e$  and on the corner  $N_c$ . Depending on the localization of each site in the crystal lattice, it is necessary to specify the number of interactions between a molecule and its first-neighbors which are denoted as  $q_i$  and the number of interactions between the molecules and the environment (surface pending links) which is denoted  $z_i$ . The present model, therefore, involves various local situations, and the Hamiltonian can finally be re-expressed as follows:

$$H = \frac{\Delta - k_B T \ln g}{2} \sum_{i=1}^{N_T} \sigma_i + \sum_{i=1}^{N_T} \frac{-2\Gamma q_i \langle \sigma \rangle - 2z_i L}{2} \sigma_i = - \sum_{i=1}^{N_T} h_i \sigma_i \quad (5)$$

where

$$h_i = - \frac{\Delta - k_B T \ln g - 2\Gamma q_i \langle \sigma \rangle - 2z_i L}{2}. \quad (6)$$

It is worth noticing that in Eq. (6), the quantity  $z_i L$  represents the extra-outer ligand field  $L_i$  introduced in Eq. (1). The characteristics of each site are listed in Table 1 for the case  $N_x, N_y$  and  $N_z \geq 3$  and in Table 2 for the case  $N_x \geq 3$ ,  $N_y \geq 3$  and  $N_z = 2$ . The case  $N_z = 1$  amounts to studying a 2D SCO nanoparticle and this case has previously been studied by Allal *et al.* [21].

## 2.1 Partition function, mean-field free energy and equation of state

The total partition function of this inhomogeneous mean-field system containing  $N_b$ ,  $N_c$ ,  $N_e$  and  $N_s$  molecules belonging respectively to bulk, corner, edge and surface regions writes

$$Z = Z_b^{N_b} Z_c^{N_c} Z_e^{N_e} Z_s^{N_s}. \quad (7)$$

The expressions of the partition functions for bulk ( $Z_b$ ), corner ( $Z_c$ ), edge ( $Z_e$ ) and surface ( $Z_s$ ) sites-have the general form:

$$Z_\alpha = 2 \cosh \beta \left( \frac{\Delta - k_B T \ln g - 2\Gamma q_\alpha \langle \sigma \rangle - 2z_\alpha L}{2} \right) \quad (8)$$

where  $\alpha = b, c, e, s$ , takes its corresponding value according to the position of the site in the lattice, while the average magnetization of site  $\alpha$  is calculated in the canonical statistics as follows:

$$\langle \sigma_x \rangle = \frac{1}{Z} \sum_{\{\sigma\}} \sigma_x \prod_{\alpha=e,b,c,s} e^{-\beta E_\alpha} \quad (9)$$

where  $E_\alpha$  is the total energy of region  $\alpha$  and  $\{\sigma\} = \{\sigma_b, \sigma_c, \sigma_e, \sigma_s\}$  stands for all spin configurations of bulk, corner, edge and surface. According to Eq. (5), the energy  $E_\alpha$  writes:

$$E_\alpha = - \sum_{i_\alpha=1}^{N_\alpha} h_\alpha \sigma_{i_\alpha}. \quad (10)$$

Since all regions are independent of each other, Eq. (7) can be factorized. So, the average magnetization of the bulk is written under the following form:

$$\langle \sigma_b \rangle = \frac{1}{Z_b^{N_b}} \sum_{\{\sigma_b\}} \sigma_b \prod_{i_b}^{N_b} e^{\beta h_b \sigma_b} \quad (11)$$

Developing further the equation leads to the following expression:

$$\langle \sigma_b \rangle = - \frac{\sinh \beta \left( \frac{\Delta - k_B T \ln g - 2\Gamma q_b \langle \sigma \rangle - 2z_b L}{2} \right)}{\cosh \beta \left( \frac{\Delta - k_B T \ln g - 2\Gamma q_b \langle \sigma \rangle - 2z_b L}{2} \right)} \quad (12)$$

This formulation can be generalized to all regions through the general expression:

$$\langle \sigma_\alpha \rangle = - \tanh \beta \left[ \frac{\Delta - k_B T \ln g - 2\Gamma q_\alpha \langle \sigma \rangle - 2z_\alpha L}{2} \right], \alpha = b, c, e, s. \quad (13)$$

The four equations obtained previously in Eq. (13) have to be combined with the relation giving the average order parameter of the system, which is obtained as averaged quantity over the four types of regions with their proportions:

$$\langle \sigma \rangle = \frac{N_b \langle \sigma_b \rangle + N_c \langle \sigma_c \rangle + N_e \langle \sigma_e \rangle + N_s \langle \sigma_s \rangle}{N_{tot}} = \frac{1}{N_{tot}} \sum_{\alpha} N_{\alpha} \langle \sigma_{\alpha} \rangle. \quad (14)$$

Finally, only one order parameter remains in the system, which is solved by bisection technique using Eqs. (13) and (14) which define a self-consistent problem.

According to the lattice symmetry and topology, the following self-consistent equations are detailed for some concrete cases of simple cubic symmetry.

### Case $N_x, N_y$ and $N_z \geq 3$

- for the bulk  $\langle \sigma_b \rangle = \tanh \left( -\frac{\Delta - k_B T \ln(g) - 2 \times 6 \Gamma \langle \sigma \rangle}{2 k_B T} \right)$
- for the surface  $\langle \sigma_s \rangle = \tanh \left( -\frac{\Delta - k_B T \ln(g) - 2 \times 5 \Gamma \langle \sigma \rangle - 2 L}{2 k_B T} \right)$  (15)
- for the edge  $\langle \sigma_e \rangle = \tanh \left( -\frac{\Delta - k_B T \ln(g) - 2 \times 4 \Gamma \langle \sigma \rangle - 2 \times 2 L}{2 k_B T} \right)$
- and for the corner  $\langle \sigma_c \rangle = \tanh \left( -\frac{\Delta - k_B T \ln(g) - 2 \times 3 \Gamma \langle \sigma \rangle - 2 \times 3 L}{2 k_B T} \right)$

### Case $N_x$ and $N_y \geq 3$ and $N_z = 2$

- for the surface  $\langle \sigma_s \rangle = \tanh \left( -\frac{\Delta - k_B T \ln(g) - 2 \times 5 \Gamma \langle \sigma \rangle - 2 \times 1 L}{2 k_B T} \right)$
- for the edge  $\langle \sigma_e \rangle = \tanh \left( -\frac{\Delta - k_B T \ln(g) - 2 \times 4 \Gamma \langle \sigma \rangle - 2 \times 2 L}{2 k_B T} \right)$  (16)
- and for the corner  $\langle \sigma_c \rangle = \tanh \left( -\frac{\Delta - k_B T \ln(g) - 2 \times 3 \Gamma \langle \sigma \rangle - 2 \times 3 L}{2 k_B T} \right)$

The set of the above self-consistent equations, which are of classical type  $\langle \sigma \rangle = \tanh f(\langle \sigma \rangle)$ , are solved numerically using the bisection method.

The high-spin fraction,  $N_{HS}$ , which is the probability to occupy the (HS) state is deduced from:

$$N_{HS} = \frac{1 + \langle \sigma \rangle}{2}. \quad (17)$$

## 2.2 The transition temperature and the nature of the transition

To understand the main types of spin transition curve (gradual, stepwise one with two or three steps, with hysteresis or incomplete spin transition) and to predict the presence or the absence of hysteresis loops, it is essential to be able to compare the two temperatures  $T_{OD}$  and

$T_{eq}$ . Indeed, the occurrence condition of a first-order phase transition with a hysteresis cycle is  $T_{OD} > T_{eq}$  whereas a gradual transition is observed when  $T_{OD} < T_{eq}$ .

In the pure Ising model,  $T_{OD}$  is the order-disorder (or Curie) temperature, obtained by putting  $\Delta/k_B = 0$ ,  $L/k_B = 0$  and  $g = 1$  ( $\ln(g) = 0$ ) in the Hamiltonian of Equation (1). Taking into account the different types of sites, the order-disorder temperature of the system  $T_{OD}$  can be expressed as follows:

$$T_{OD} = \frac{N_b T_{OD}^b + N_s T_{OD}^s + N_e T_{OD}^e + N_c T_{OD}^c}{N_{tot}} \quad (18)$$

and  $T_{OD}^b$ ,  $T_{OD}^s$ ,  $T_{OD}^e$ ,  $T_{OD}^c$  are respectively the order-disorder temperature of bulk, surface, edge and corner particles.

The different values of  $N_b$ ,  $N_s$ ,  $N_e$ ,  $N_c$  and  $T_{OD}^b$ ,  $T_{OD}^s$ ,  $T_{OD}^e$ ,  $T_{OD}^c$  obtained in the framework of the approximations, are gathered in table 3 and 4 as a function of the lattice size.

A null total effective ligand-field leads to the equilibrium temperature  $T_{eq}$  of the system and is defined as the temperature for which the (HS) fraction is equal to 1/2. For a cubic lattice with size  $N_x \times N_y \times N_z$ ,  $T_{eq}$  is the solution to the following equation:

$$\frac{\Delta - k_B T_{eq} \ln g}{2} \times N_b + \frac{\Delta - k_B T_{eq} \ln g - 2L}{2} \times N_s + \frac{\Delta - k_B T_{eq} \ln g - 4L}{2} \times N_e + \frac{\Delta - k_B T_{eq} \ln g - 6L}{2} \times N_c = 0 \quad (19)$$

The solution of this linear equation, proposed by Muraoka *et al.* [29] gives the following analytical expression for the equilibrium temperature:

$$T_{eq} = \frac{N_b T_{eq}^b + N_s T_{eq}^s + N_e T_{eq}^e + N_c T_{eq}^c}{N_{tot}} \quad (20)$$

where  $T_{eq}^b$ ,  $T_{eq}^s$ ,  $T_{eq}^e$  and  $T_{eq}^c$  are the respective equilibrium temperature of bulk, surface, edges and corners and whose analytical expressions are:

$$T_{eq}^b = \frac{\Delta}{k_B \ln(g)} \quad T_{eq}^s = \frac{\Delta - 2L}{k_B \ln(g)} \quad T_{eq}^e = \frac{\Delta - 4L}{k_B \ln(g)} \quad T_{eq}^c = \frac{\Delta - 6L}{k_B \ln(g)} \quad (21)$$

Considering a cubic system  $N_x$ ,  $N_y$  and  $N_z$  are such that  $N_x = N_y = N_z = N$ , and finally:

$$N_b = (N - 2)^3, N_s = 6(N - 2)^2, N_e = 12(N - 2) \text{ and } N_c = 8.$$

Replacing the analytical expressions of  $N_b$ ,  $T_{eq}^b$ ,  $N_s$ ,  $T_{eq}^s$ ,  $N_e$ ,  $T_{eq}^e$ ,  $N_c$  and  $T_{eq}^c$  in equation (20), the expression of the equilibrium temperature becomes :

$$T_{eq} = \frac{\Delta/k_B}{\ln(g)} - \frac{12L/k_B}{N \ln(g)}. \quad (22)$$

It means that, for an infinite size system with  $N \rightarrow \infty$ ,  $L/k_B$  and  $\ln(g)$  being constant,  $T_{eq}$  tends towards the equilibrium temperature of the bulk  $T_{eq}^b = \frac{\Delta/k_B}{\ln(g)}$ .

To be able to also study the effect of an external isotropic pressure  $P$  on the properties of the SCO nanoparticle under isothermal conditions, the ligand field energy  $\Delta$  is replaced in the Hamiltonian by  $\Delta + \Delta V \times P$ , where  $\Delta V = V_{HS} - V_{LS}$  is the volume change per molecule of the material between the (HS) and the (LS) states.

Taking into account the pressure effect, the Hamiltonian is modified in the following form [6-7]:

$$H = \frac{\Delta + \Delta V \times P - k_B T \ln g - 2\Gamma q \langle \sigma \rangle - 2zL}{2} \sum_{i=1}^{N_T} \sigma_i \quad (23)$$

and the analytical expressions of the transition temperatures associated with the bulk, the surface, the edge and the corner are adapted as:

$$T_{eq}^b = \frac{\Delta + \Delta V \times P}{k_B \ln(g)} \quad T_{eq}^s = \frac{\Delta + \Delta V \times P - 2L}{k_B \ln(g)} \quad T_{eq}^e = \frac{\Delta + \Delta V \times P - 4L}{k_B \ln(g)} \quad T_{eq}^c = \frac{\Delta + \Delta V \times P - 6L}{k_B \ln(g)} \quad (24)$$

### 3. NUMERICAL RESULTS AND DISCUSSION

To explore in details the thermal and pressure properties of a 3D SCO nanoparticle, the behavior of the average magnetization  $\langle \sigma \rangle$  and thus of the (HS) fraction is simulated in the frame of the (LMFA) as a function of temperature and pressure thanks to various parameters whose values are chosen in such a way that they correspond to the class of FeII SCO compounds that exhibit cooperative spin transitions very close to ambient temperature.

#### 3.1 Three states and three steps as a function of temperature

##### 3.1.1 Size effects

The thermodynamic parameters of the  $[\text{Fe}(\text{Htrz})_2(\text{trz})](\text{BF}_4)_2$  spin crossover complex [30] have been used in the numerical simulations. For this compound, the molar entropy change is  $\Delta S \approx 70.25$  J/K/mol, which leads to  $\ln(g) = \Delta S/R \approx 8.45$ .  $R$  is the perfect gas constant and the energy gap  $\Delta/k_B = 3126$  K. Thus, in a non-interacting system, the equilibrium temperature at which the fractions of (LS) and (HS) are equal is  $T_{eq} = \frac{\Delta}{k_B \ln(g)} \approx 370$  K and it is also the transition temperature in the bulk as it can be seen in Table 5 below.

For various SCO nanoparticle sizes, the thermal behavior of the (HS) fraction as a function of temperature is reported in Fig. 3. Positive “ferromagnetic-like” interactions  $\Gamma$  and positive interactions  $L$  between the molecules at the surface and the surrounding matrix are considered.

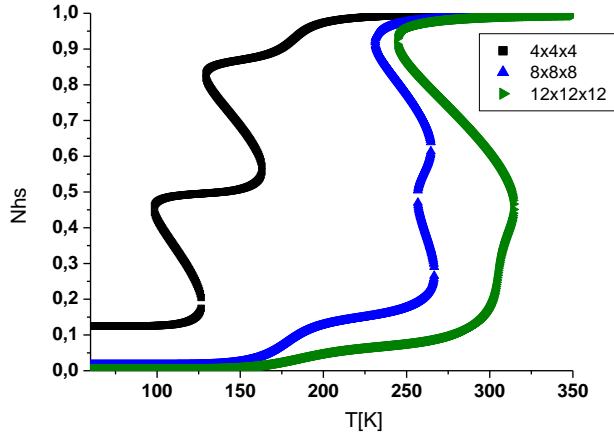


**Fig. 3.** Thermal evolution of the (HS) molar fraction in a 3D cubic lattice embedded in a matrix for different cubic lattice sizes:  $4 \times 4 \times 4$  (black squares),  $8 \times 8 \times 8$  (blue up triangles),  $12 \times 12 \times 12$  (green right triangles). The computational parameters are  $\Delta/k_B=3126$  K,  $\Gamma/k_B=150$  K,  $L/k_B=650$  K and  $\ln(g)=8.45$ .

It is interesting to observe that upon reducing the lattice size, a three-step transition emerges. This behavior has been experimentally well documented in 2D and 3D SCO compounds [5, 31]. It also appears that the transition temperature is shifted downward and that the low-temperature residual (HS) fraction is increased. More precisely, in the case of a  $4 \times 4 \times 4$  nanoparticle, the transition temperature which corresponds to  $n_{HS} = 1/2$  is equal to  $(T_{eq}^e + T_{eq}^s)/2 \approx 139$  K. For the  $8 \times 8 \times 8$  lattice, the transition temperature is equal to  $\approx 258$  K and tends towards  $(T_{eq}^s + T_{eq}^b)/2 = 292$  K. In the case of the  $12 \times 12 \times 12$  system, the equilibrium temperature tends towards that of the bulk ( $\approx 370$  K) and the curve almost looks like a single hysteresis loop.

It clearly appears that shrinking the size can have significant consequences. The surface to volume ratio increases and as part of a heat-induced transition, this leads on the one hand to a change in the transition temperature by several tens of Kelvins and on the other hand to a drastic change in the type of spin transition.

To pay particular attention to the  $8 \times 8 \times 8$  size nanoparticle, as shown in Fig. 4, an enlarged view of the domain which extends from 225 K to 275 K exhibits, on one hand, the presence of an intermediate plateau (a mixture of (LS) and (HS) configurations) obtained between 256 K and 264 K with  $N_{hs} \approx 0,55$  and on the other hand two hysteresis loops. The first one denoted H1 is in the range 256-267 K with  $N_{hs}=0.15$  to 0.55 which implies that, at 225 K, a small fraction of the SCO molecules are already in the HS state and the second one is in the range 231-265 K with  $N_{hs}=0.55$  to 0.1.

The overlap of the two hysteresis loops H1 and H2 leads to the simultaneous presence of three stable states in the temperature range  $T_2-T_1=9$  K. The thermal evolution of the (HS) fraction reports on the following intramolecular processes (LS)  $\leftrightarrow$  (LS) + (HS) for the H1 hysteresis loop and (LS) + (HS)  $\leftrightarrow$  (HS) for the H2 hysteresis loop. The switching from one state to

another presents particularly interesting potentials applications in the field of information storage.

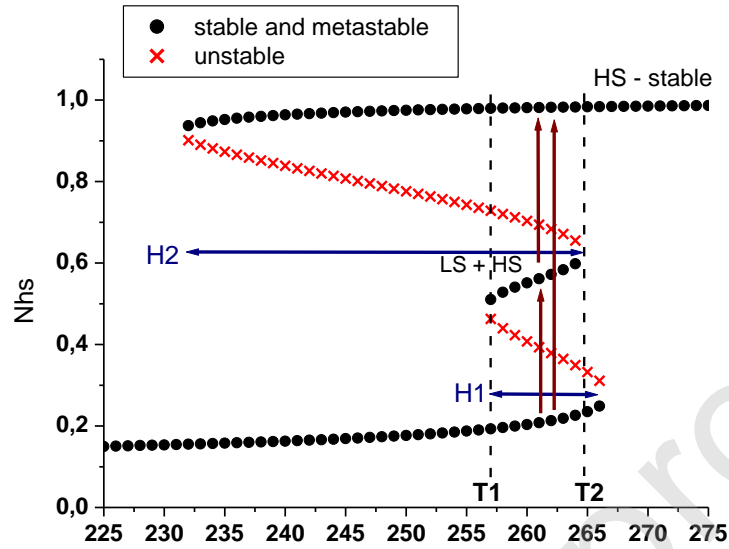
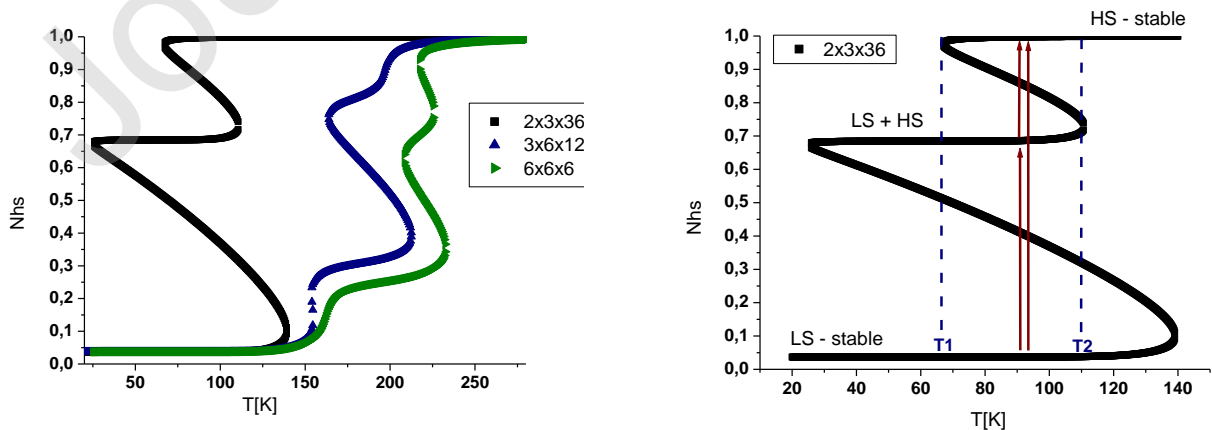


**Fig. 4.** Enlarged view of the evolution of the (HS) molar fraction as a function of temperature. Three states hysteresis loop in a 3D SCO cubic lattice with size  $8 \times 8 \times 8$ : stable and metastable regions (filled black circles) and unstable regions (red crosses). The computational parameters are  $\Delta/k_B=3126$  K,  $\Gamma/k_B=150$  K,  $L/k_B=650$  K and  $\ln(g)=8.45$ .

### 3.1.2 Shape effects

In this subsection, the thermal-dependence of the (HS) fraction is analyzed for different 3D lattice shapes comprising 216 (see Fig. 5) and 512 SCO (see Fig. 6) molecules. For start, a cubic lattice is considered, and a progressive increment along the length is made until an elongated parallelepiped is obtained. For a  $N_x \times N_y \times N_z$  lattice, a ratio parameter  $t$  is defined such that  $t = (N_c + N_e + N_s)/N_T$  is the ratio between outline and total numbers of molecules.



(a) (b)  
**Fig. 5.** Thermal evolution of the (HS) molar fraction for a 3D SCO system comprising 216 molecules (a) for different lattice shapes:  $2 \times 3 \times 36$  (black squares),  $3 \times 6 \times 12$  (blue up triangles),  $6 \times 6 \times 6$  (left green triangles), (b)  $2 \times 3 \times 36$  lattice shape: enlarged view of the two steps and the three states hysteresis loop. The computational parameters are  $\Delta/k_B=3126$  K,  $\Gamma/k_B=150$  K,  $L/k_B=650$  K and  $\ln(g)=8.45$ .

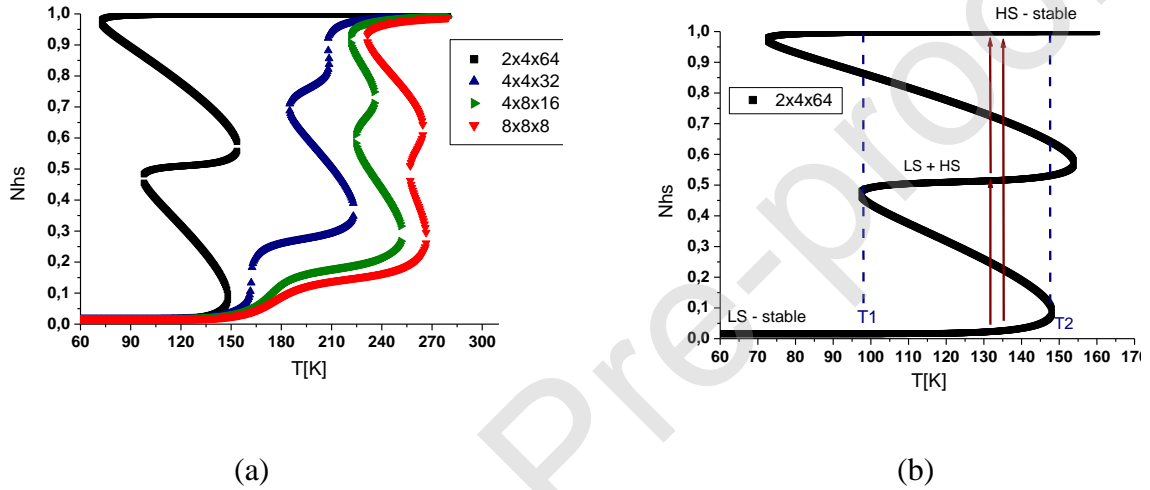


**Fig. 6.** Thermal evolution of the HS molar fraction for a 3D SCO system comprising 512 molecules (a) for different lattice shapes:  $2 \times 4 \times 64$  (black squares),  $4 \times 4 \times 32$  (blue up triangles),  $4 \times 8 \times 16$  (left green triangles),  $8 \times 8 \times 8$  (down red triangles). (b)  $2 \times 4 \times 64$  lattice shape: enlarged view of the two steps and the three states hysteresis loop. The computational parameters are  $\Delta/k_B=3126$  K,  $\Gamma/k_B=150$  K,  $L/k_B=650$  K and  $\ln(g)=8.45$ .

For elongated parallelepiped systems, the spin transition presents two hysteresis loops and occurs in two well-defined steps from  $N_{hs}=0-0.5$  for the first one, and from  $N_{hs}=0.5-1$  for the second one. The two hysteresis loops have an overlap over a temperature interval of  $\approx 50$  K for the  $2 \times 4 \times 64$  system, and of  $\approx 43$  K for the  $2 \times 3 \times 36$  system which is only slightly different. In contrast, the two-step spin transition is shifted to lower temperatures for the smaller system  $2 \times 3 \times 36$ .

In the case of the  $2 \times 3 \times 36$  nanoparticle, the equilibrium temperature for which  $N_{hs}=1/2$  is approximately 66 K and corresponds as can be seen in Table 6 to the equilibrium temperature of the edge  $T_{eq}^e$ . In the case of the  $2 \times 4 \times 64$  nanoparticle, the equilibrium temperature is approximately 120 K and is close to  $(T_{eq}^e + T_{eq}^s)/2$  as can be seen in Table 7.

### 3.1.3 Three steps

These calculations highlight three steps associated with three hysteresis loops H1, H2 and H3 (Fig. 7) in the heating mode as well as in the cooling mode. Similar behavior is obtained in the case of  $6 \times 6 \times 6$  SCO system by increasing the value of its interaction parameter  $L/k_B$  up to 775 K compared to the calculations of the two previous subsections. Indeed, it is noticeable that increasing the value of parameter  $L/k_B$  increases the width of hysteresis H2 and with a shift towards lower temperatures, which leads to the presence of two well defined intermediate bearings.

Changing the value of the parameter  $L$  would amount experimentally to modify the effect of the matrix.

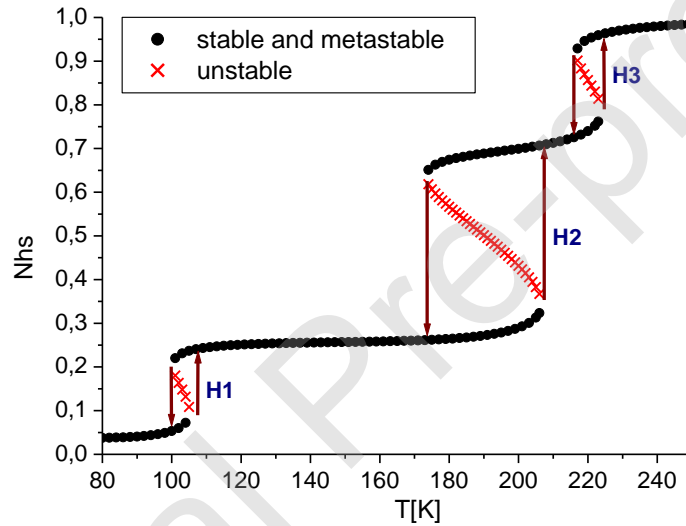


**Fig. 7.** Thermal evolution of the (HS) molar fraction and three hysteresis loops in a 3D SCO cubic lattice with size  $6 \times 6 \times 6$ . The computational parameters are  $\Delta/k_B=3126$  K,  $\Gamma/k_B=150$  K,  $L/k_B=775$  K and  $\ln(g)=8.45$ .

### 3.2 Three states and three steps under pressure

In this section, focus is paid on the effect of applying external pressure under isothermal conditions in 3D SCO compounds. As represented in Fig. 8, in the case of  $6 \times 6 \times 6$  nanoparticle, switching from the (HS) state to the (LS) state is achievable with two steps and three states phenomenon. The coexistence of these three states is linked to the presence of two superimposed hysteresis loops which overlap in the pressure interval  $P_2-P_1=14$  Mpa. The first loop denoted H1 extends in the range 227-245 MPa with values of  $N_{hs}$  between 0.96 and 0.75 and the second one in the range 190-260 MPa with values of  $N_{hs}$  between 0.63 and 0.25. This means that this two-step behavior is incomplete and that a residual fraction of (HS)

configurations remains beyond 260 Mpa. This residual fraction of (HS) states progressively decreases and finally vanishes when the pressure reaches around 800 MPa. An intermediate plateau which corresponds to a mixture of (HS) and (LS) configurations is obtained in the pressure range 227 and 260 MPa for  $N_{hs}$  between 0,75 and 0,64.

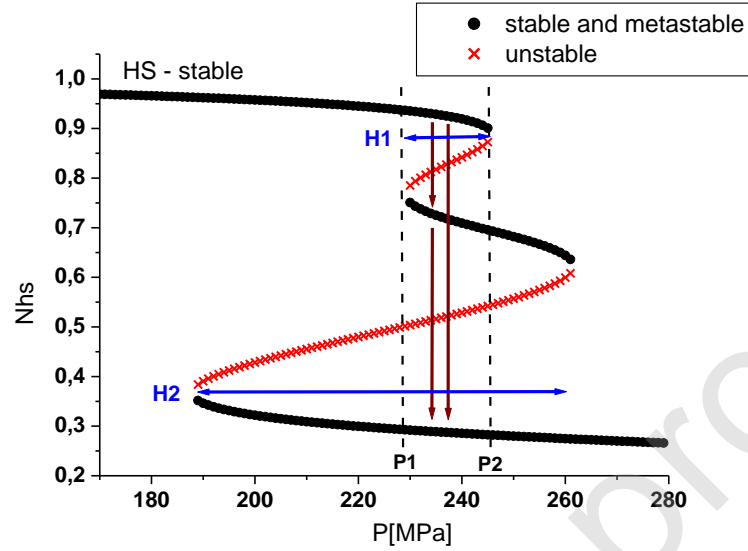


**Fig. 8.** Pressure-dependence of the (HS) fraction in isothermal conditions ( $T=270$  K) and three states hysteresis loops in a SCO system with size  $6 \times 6 \times 6$ . The computational parameters are:  $\Delta/k_B = 3126$  K,  $\Gamma/k_B = 155$  K,  $L/k_B = 650$  K,  $\ln(g) = 8.45$ ,  $\Delta V = 100 \text{ \AA}^3$ .

The increase in the values of the interaction parameters  $\Gamma/k_B$  and  $L/k_B$  accentuates respectively the width of the hysteresis loops H1 and H2 and shifts them towards high pressures. In addition, H1 and H2 are well separated from each other and a three-step behavior is obtained.

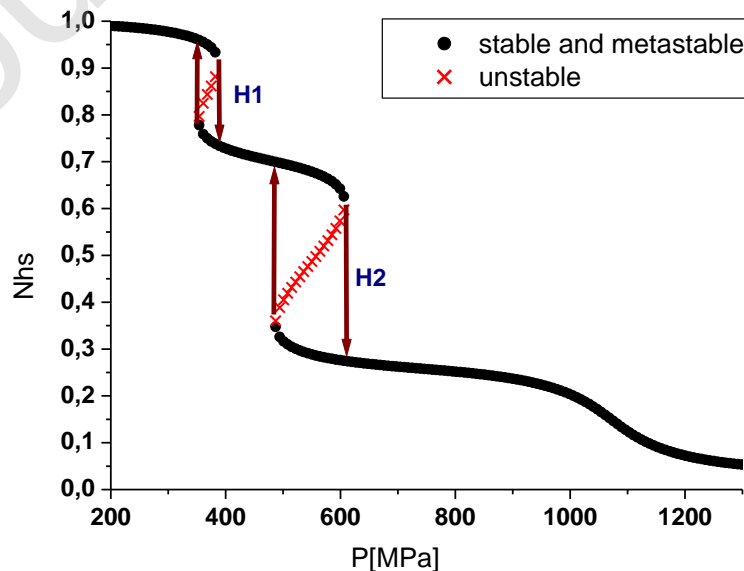


**Fig. 9.** Pressure-dependence of the (HS) fraction under isothermal conditions ( $T=270$  K) and three steps behavior in a SCO system with size  $6 \times 6 \times 6$ . The computational parameters are:  $\Delta/k_B = 3126$  K,  $\Gamma/k_B = 180$  K,  $L/k_B = 950$  K,  $\ln(g) = 8.45$ ,  $\Delta V = 100 \text{ \AA}^3$ .

#### 4 CONCLUSION

To summarize, this work demonstrates that the local mean-field approximation (LMFA) is well adapted to study interacting-molecules in 3D-SCO system of nanoparticles where the total amount of molecules at the surface are equivalent or even more than the molecules in the bulk. In fact, LMFA allows to discriminate the number of neighbors for the different situations of the molecules: at the surface, edge, corner and at the bulk.

By this approximation, the action of the environment on the molecules at the surface is also studied, and the numerical results show that the three steps LS-HS thermal hysteresis is obtained when this local environment is taken into account as an additional interaction considering the different environment for external molecules (surface, edge and corner).

Given that, LMFA and matrix effects are taken into account, it could be claimed that the thermodynamic interplay between the non-bulk (i.e. surface, edge, and corner), and bulk molecules give rise to two or even multi-step transitions.

Using local mean field approximations, the effect of different sizes (Fig. 3) and different shapes for the same number of molecules (Fig. 5 and 6) on the spin transition could be easily determined, and thus could be used to establish the thermal behavior of the total spin fraction on different cubic and cuboid lattices.

When table 5 is considered, a certain pattern is appearing, showing that as the lattice size is being reduced, the equilibrium temperature is shifting towards lower temperatures. This behavior is certainly consistent with the 2D lattice observations, thus confirming that non-bulk entities (edges and surfaces) play a major role in determining the equilibrium temperature for smaller lattices. Similarly, for bigger lattices, it is the ratio of bulk to surface molecules which determines the fate of the equilibrium temperature for that particular lattice architecture, as it can be seen from table 6 and 7. This interplay between surface and bulk molecules on the characteristics of the thermal transition is very interesting and deserves to be investigated more deeply in future works.

The impact of specific conditions such as the effect of interaction parameter  $L/k_B$  on SCO nanoparticles has been investigated in a 3-D model, which is studied in Fig. 7. It clearly demonstrates when compared with results in Fig. 5, that keeping everything else constant and just increasing the interaction parameter will lead to a decrease in the transition temperature

and an increase in thermal hysteresis width for the same lattice size. Thus these definite behaviors indicate that under specific boundary conditions, the system might act as if it is under negative pressure, which justifies the downwards shift in the equilibrium temperature.

The widening of the hysteresis widths and the generation of a three-step transition, when either lattice sizes are reduced, or its shapes are changed in order to change the bulk to surface molecule ratios, suggest the role of interplay between the equilibrium temperature variation and the expected Curie temperature, arising from a pure Ising model.

A three-state behavior for a 6x6x6 system has also been obtained by using calorimetric typical values of the SCO. The effect of external pressure on 3D spin-crossover compounds has been analyzed with particular attention paid to the effect of the interactions between bulk and non-bulk molecules and their local environment, which were taken into account in the coupling parameter,  $L$ . As shown in Fig. 8 and Fig. 9, the variation in the coupling parameter leads to a variation in the hysteresis behaviors, due to the applied pressure.

The ligand field at the surface of the lattice is weaker than that of the bulk, due to the matrix's contribution. This indicates the role played by the surface effect on the spin transition due to applied pressure, as soon as both surface and bulk effects are combined by increasing the coupling parameter. The effect of pressure will be clearly different on the surface and the volume, and so its impact on the transition pressure will depend on the ratio of surface to volume entities. This explains the stabilization of HS states when the coupling parameters and the long range-short range interactions for the 6x6x6 lattice are increased. In the end, a two-step Pressure phase transition result is depicting the interaction between molecules, and the competition between  $\Delta$ , the energy Gap between HS and LS state, that favors LS state and the hydrostatic pressure and the matrix interaction that favors HS. This matrix effect plays an opposite role to a typical applied hydrostatic pressure because it favors the HS state.

These results demonstrated the key role played by surface effects on the phase stability and transition of SCO nano-objects, thus surface relaxations and its mechanism must be considered as the nanoscale is approached. By taking all these factors into account a three-state electronic storage device can be proposed.

CRedit author statement

**Catherine Cazelles:** Software, Writing - Original Draft.

**Yogendra Singh :** Software, Writing - Original Draft.

**Jorge Linares:** Conceptualization, Methodology, Project administration, Writing - Review & Editing, Software

**Pierre-Richard Dahoo:** Software, Writing - Review & Editing,

**Kamel Boukheddaden :** Conceptualization, Methodology, Project administration, Writing - Review & Editing

We confirm that the manuscript has been read and approved by all named authors.

We confirm that the order of authors listed in the manuscript has been approved by all named authors.

### Declaration of interests

The authors declare that they have no known competing financial interests or personal relationships that could have appeared to influence the work reported in this paper.

### Acknowledgments

CHAIR Materials Simulation and Engineering of UVSQ-UPSAY, the French "Ministère de la Recherche", the Université de Versailles St. Quentin-en-Yvelines, Université Paris-Saclay, CNRS and ANR BISTA-MAT (ANR-12-BS07-0030-01) are warmly acknowledged for the financial support.

### REFERENCES

- [1] E. Konig, *Struct. Bond.* 76 (1991) 51–152.
- [2] O. Kahn, *Solid State Mater. Sci.* 1 (1996) 547–554.
- [3] P. Gutlich, *Struct. Bond.* 44 (1981) 83–195.
- [4] O. Kahn, J.P. Launay, *Chemtronics.* 3 (1988) 140–151.
- [5] J. E. Clements, J. R. Price, S. M. Neville, C. J. Kepert, *German Chemical Society.* 55 (48) (2016) 15105–15109.
- [6] F. Varret, S.A. Salunke, K. Boukheddaden, A. Bousseksou, E. Codjovi, *Comptes Rendus Chimie.* 6 (3) (2003) 385–394.
- [7] R. Boca, I. Salitros, J. Kozisek, J. Linares, J. Moncol, F. Renz, *Dalton Transactions.* 39 (9) (2010) 2198–2200.
- [8] H. Constant-Machado, A. Stancu, J. Linares, F. Varret, *IEEE Transactions on Magnetism* 34 (4) (1998) 2213–2219.
- [9] J. Jeftic, A. Hauser, *J. Phys. Chem. B.* 101 (1997) 10262–10270.
- [10] G. Molnar, V. Niel, J.A. Real, L. Dubrovinsky, A. Bousseksou, J.F. McGarvey, *J. Phys. Chem. B.* 107 (2003) 3149–3155.
- [11] A. Rotaru, J. Linares, F. Varret, E. Codjovi, A. Slimani, R. Tanasa, C. Enachescu, A. Stancu and J. Haasnoot. *Phys. Rev. B.* 83 (22) (2011) 224107.
- [12] A. Bousseksou, K. Boukheddaden, M. Goiran, C. Consejo, M.L. Boillot, J.P. Tuchagues, *Phys. Rev. B.* 65 (2002) 172412.

- [13] S. Decurtins, P. Gutlich, C.P. Kohler, H. Spiering, A. Hauser, *Chem. Phys. Lett.* 105 (1984) 1–4.
- [14] P. Gütlich, A. Hauser, H. Spiering, *Angew. Chem. Int. Edit.* 33 (1994) 2024–2054.
- [15] S. Bonhommeau, G. Molnar, A. Galet, A. Zwick, J.A. Real, J.F. McGarvey, A. Bousseksou, *Angew. Chem. Int. Edit.* 44(2005) 4069–4073.
- [16] N.O. Moussa, G. Molnar, S. Bonhommeau, A. Zwick, S. Mouri, K. Tanaka, J.A. Real, A. Bousseksou, *Phys. Rev. Lett.* 94 (2005) 107205.
- [17] S. Decurtins, P. Gutlich, K.M. Hasselbach, A. Hauser, H. Spiering, *Inorg. Chem.* 24 (1985) 2174–2178.
- [18] C. Enachescu, N. Menendez, E. Cadjovi, J. Linares, F. Varret, A. Stancu, *Physica B: Condensed Matter.* 306 (1) (2001) 155–160.
- [19] H. Oubouchou, Y. Singh, K. Boukheddaden, *Phys. Rev. B.* 98 (2018) 014106.
- [20] A. Rotaru, M. Dîrtu, C. Enachescu, R. Tanasa, J. Linares, A. Stancu, Y. Garcia, *Polyhedron.* 28 (2009) 2531–2536.
- [21] S.E.Allal, J. Linares, K. Boukheddaden, P. R. Dahoo, F. de Zela, *Journal of Physics: CS.* 936 (2017) 012052.
- [22] J. Wajnfłasz, R. Pick, *J. Phys.Colloques.* 32(C1) (1971) 91–92.
- [23] A. Bousseksou, J. Nasser, J. Linares, K. Boukheddaden, F. Varret, *J. Phys. I France.* 2(7) (1992) 1381–1403.
- [24] B. Hoo, K. Boukheddaden, F. Varret, *Europ. Phys. J. B.* 17 (2000) 449–457.
- [25] J. Linares, H. Spiering, F. Varret, *Eur. J. Phys. B.* 10 (1999) 271–275.
- [26] K. Boukheddaden, J. Linares, H. Spiering, F. Varret, *Europ. Phys. J. B.* 15 (2000) 317–326.
- [27] J. Linares, C.M. Jureschi, K. Boukheddaden, *Magnetochemistry.* 2(2) (2016) 24.
- [28] D. Chiruta, J. Linares, M. Dimian, Y. Alayli, Y. Garcia, *Eur. J. Inorg. Chem.* 29 (2013) 5086–5093.
- [29] A. Muraoka, K. Boukheddaden, J. Linares, F. Varret, *Phys. Rev. B.* 84 (2011) 054119.
- [30] J. Krober, J.P. Audière, R. Claude, O. Kahn, J. Hassnoot, F. Grolière, C. Jay, A. Bousseksou, J. Linares, F. Varret, A. Gonthier-Vassal, *Chem. Mater.* 6 (1994) 1404.
- [31] N.F. Sciortino, K.R. Scherl-Gruenwald, G. Chastanet, G.J. Halder, K.W. Chapman, J.F. Létard, C.J. Kepert, *Angewandte Chemie.* 124 (40) (2012) 10301–10305.

**Table 1.** Ligand field contributions as a function of the molecule's position in the lattice for the case  $N_x, N_y$  and  $N_z \geq 3$

site	bulk	surface	edge	corner
$q_i$	6	5	4	3
$z_i$	0	1	2	3
ligand-field	$\frac{\Delta - k_B T \ln g}{2}$	$\frac{\Delta - k_B T \ln g - 2L}{2}$	$\frac{\Delta - k_B T \ln g - 4L}{2}$	$\frac{\Delta - k_B T \ln g - 6L}{2}$

**Table 2.** Ligand-field contribution as a function of the molecule's position in the lattice for the case  $N_x$  and  $N_y \geq 3$  and  $N_z = 2$ .

site	bulk	surface	edge	corner
$q_i$	0	5	4	3
$z_i$	0	1	2	3
ligand-field	-	$\frac{\Delta - k_B T \ln g - 2L}{2}$	$\frac{\Delta - k_B T \ln g - 4L}{2}$	$\frac{\Delta - k_B T \ln g - 6L}{2}$

**Table 3.** Number of molecules in the bulk, surface, edge and corner and their corresponding lattice coordination number (number of first-nearest neighbors),  $q$ , as well as their corresponding order-disorder temperature,  $T_{OD}$ , for a cubic lattice with  $N_x, N_y$  and  $N_z \geq 3$ .

site	number of molecules	number of first-neighbors $q$	$T_{OD}$
bulk	$N_b = (N_x - 2) \times (N_y - 2) \times (N_z - 2)$	6	$6\Gamma/k_B$
surface	$N_s = (N_x - 2) \times (N_z - 2) \times 2 + (N_x - 2) \times (N_y - 2) \times 2 + (N_y - 2) \times (N_z - 2) \times 2$	5	$5\Gamma/k_B$
Edge	$N_e = (N_x - 2) \times 4 + (N_y - 2) \times 4 + (N_z - 2) \times 4$	4	$4\Gamma/k_B$
corner	$N_c = 8$	3	$3\Gamma/k_B$

**Table 4.** Number of molecules, of first-neighbors and value of  $T_{OD}$  as a function of the molecules' localization in a cubic lattice when  $N_x$  and  $N_y \geq 3$  and  $N_z = 2$ .

site	number of molecules	number of first-neighbors $q$	$T_{OD}$
bulk	$N_b = 0$	-	-
surface	$N_s = (N_x - 2) \times (N_y - 2) \times N_z$	5	$5\Gamma/k_B$
Edge	$N_e = (N_x - 2) \times 4 + (N_y - 2) \times 4$	4	$4\Gamma/k_B$
corner	$N_c=8$	3	$3\Gamma/k_B$

**Table 5.** Order-disorder and equilibrium temperatures calculated for different sizes of 3D cubic SCO nanoparticle. The parameters are  $\Delta/k_B=3126$  K,  $\Gamma/k_B=150$  K,  $L/k_B=650$  K and  $\ln(g)=8.45$

$N_x$	$N_y$	$N_z$	$N_T$	$T_{eq}^c$	$T_{eq}^e$	$T_{eq}^s$	$T_{eq}^b$	$T_{OD}(LMFA)$	$T_{eq}(LMFA)$
4	4	4	64	-91.60	62.25	216.09	369.94	675	139.17
8	8	8	512	-91.60	62.25	216.09	369.94	787.5	254.56
12	12	12	1728	-91.60	62.25	216.09	369.94	825	293.02

**Table 6.** Order-disorder and equilibrium temperatures calculated for various shapes of 3D SCO nanoparticle comprising 216 molecules. The parameters are  $\Delta/k_B=3126$  K,  $\Gamma/k_B=150$  K,  $L/k_B=650$  K and  $\ln(g)=8.45$ .

$N_x$	$N_y$	$N_z$	$N_T$	$T_{eq}^c$	$T_{eq}^e$	$T_{eq}^s$	$T_{eq}^b$	$t$	$T_{OD}(LMFA)$	$T_{eq}(LMFA)$
2	3	36	216	-91.60	62.25	216.09	369.94	1.00	641.67	104.98
3	6	12	216	-91.60	62.25	216.09	369.94	0.81	725	190.45
6	6	6	216	-91.60	62.25	216.09	369.94	0.70	750	216.09

**Table 7.** Order-disorder and equilibrium temperatures calculated for various shapes of 3D SCO nanoparticle comprising 512 molecules. The parameters are  $\Delta/k_B=3126$  K,  $\Gamma/k_B=150$  K,  $L/k_B=650$  K and  $\ln(g)=8.45$ .

$N_x$	$N_y$	$N_z$	$N_T$	$T_{eq}^c$	$T_{eq}^e$	$T_{eq}^s$	$T_{eq}^b$	$t$	$T_{OD}(LMFA)$	$T_{eq}(LMFA)$
2	4	64	512	-91.60	62.25	216.09	369.94	1.00	670.31	134.36
4	4	32	512	-91.60	62.25	216.09	369.94	0.77	740.63	206.48
4	8	16	512	-91.60	62.25	216.09	369.94	0.67	768.75	235.33
8	8	8	512	-91.60	62.25	216.09	369.94	0.58	787.5	254.56